ELSEVIER

Polymer 40 (1999) 6789–6801

polymer

The rheological properties of polystyrene/poly(vinylmethylether) blend near the critical region and in the homogenous region

Jin Kon Kim*, Hye Won Son

Department of Chemical Engineering and Polymer Research Institute, School of Environmental Engineering,
Pohang University of Science and Technology, Pohang 790-784, Kyungbuk, Korea

Received 12 October 1998; received in revised form 15 December 1998; accepted 4 January 1999

Abstract

The rheological properties of polystyrene/poly(vinylmethylether) (PS/PVME) blend near the critical region and in the homogeneous region were investigated. The blend had a lower critical solution temperature (LCST) of 112°C obtained by a turbidity experiment using a light scattering (LS) apparatus at a heating rate of 1°C/h. Four different blend compositions (critical (30/70 PS/PVME by weight) and three off-critical (10/90, 50/50, and 70/30) as well as neat PS and PVME were prepared. For the critical composition, logarithmic plots of shear modulus (G') versus loss modulus (G'') showed temperature dependence even in the homogenous region determined by LS, while those plots become temperature independent in the homogeneous region for off-critical compositions.

Logarithmic plots of blend viscosity versus composition exhibited a negative deviation at constant temperature; however, these showed a maximum at a certain composition when the reference temperature is taken as fixed $T - T_g$ (under approximately iso-free volume condition).

Keywords: Rheological properties; PS/PVME blends; Blend viscosity

1. Introduction

The polystyrene (PS) and poly(vinylmethylether) (PVME) blend has been extensively investigated by polymer scientists [1–19], after this blend was found to exhibit a lower critical solution temperature (LCST) [9]. Some research groups have studied the phase-separation kinetics and its morphology [9–12], while others have investigated the rheological properties of PS/PVME blends near the critical temperatures as well as in the homogeneous regime [2–7].

A phase diagram of the PS/PVME blend was obtained by a light scattering and/or a small angle neutron scattering method [7,10–14] with the aid of the random phase approximation based on Flory–Huggins mean field theory. Kapnistos et al. [7] showed that the spinodal temperature of PS/PVME blend could be obtained by rheological methods of temperature sweep experiments of storage shear modulus (G') and logarithmic plots of G' versus loss shear modulus (G''). Recently, Kim et al. [18] found that the critical composition of PS/PVME blend exhibits a concentration fluctuation in the homogeneous regime close to the LCST, while off-critical composition does not exhibit the concentration fluctuation. These behaviors are consistent with results given in Ref. [7]. In addition, we showed that the extent of the concentration fluctuation in a blend near the critical temperature is inversely proportional to the absolute value of the temperature coefficient (B) in the Flory interaction parameter ($\chi = A + B/T$, where T is the absolute temperature) [18]. It is shown that the rheological properties of the blend in the phase-separated regime vary quite complicatedly with blend composition, as rheological properties depend upon the phase-separated morphology [7]. Very recently, we investigated the change in the rheological properties of PS/PVME blend with phase-separation time, depending upon the blend composition and the quenching depth [19].

Semi-empirical or theoretical predictions have long been sought which allow one to calculate the zero-shear viscosity of a miscible polymer blend (η_{ob}) in terms of the zero-shear viscosities of constituent components (η_{oi}) in the blend [20–25]. It is reported that at isothermal conditions, plots of log η_{ob} versus composition exhibit a positive deviation for blends with small difference in the glass transition (T_g) between constituent components, such as poly(methylmethacrylate) (PMMA)/poly(styrene-*co*-acrylonitrile)

---

* Corresponding author. Tel.: + 82-562-279-2276; fax: + 82-562-279-8298.

E-mail address: jkkim@postech.ac.kr (J.K. Kim)

0032-3861/99/$ - see front matter © 1999 Elsevier Science Ltd. All rights reserved.
PII: S0032-3861(99)00030-0

(PSAN) blend [21,23–25], and PS/poly(cyclohexyl methacrylate) blend [22], whereas these plots show a negative deviation for blends with large difference (say >50°C) in the T_gs between constituent components, such as PS/PVME blend [3,26], PMMA/poly(vinylidene fluoride) (PVDF) blend [20,23–25], PSAN/poly(ϵ-caprolactone) blend [27]. However, the above speculation does not always lead in the right direction. For instance, plots of log η_{ob} versus composition at isothermal conditions for PS/poly-(2,6-dimethyl-1,4-phenyleneether) (PPE) blend [28] and 1,2-polybutadiene/1,4-poly(butadine) blend [29] show a positive deviation or linear relationship, even though the difference in the T_gs of two components is very large (e.g. ~ 100°C).

According to Ougizawa and coworkers [30,31], a negative deviation from linearity in plots of log η_{ob} versus composition at isothermal condition can be expected for a blend (e.g. PMMA/PVDF) with a positive excess volume of mixing; whereas a positive deviation was found for another blend (e.g. PS/PPE) with a negative excess volume of mixing. However, there is no comprehensive theory available at the present time to include this kind of an excess volume of mixing to predict the blend viscosity [32]. In order to predict the blend viscosity from the constituent viscosities, some researchers [20–22] have developed a mixing rule that is a quadratic form with respect to the volume fraction. This kind of the mixing rule, however, contains one additional (or adjustable) parameter that cannot be obtained without measuring the viscosities of the entire blend compositions. Han and Kim [23,24] developed a molecular viscoelastic theory that enables one to predict the linear viscoelastic properties of miscible polymer blends. They showed that χ plays a very important role in determining the blend viscoelastic properties [23–25,28,33], and that theoretical predictions of the linear viscoelastic properties of the several blends, such as PMMA/PVDF, PMMA/PSAN, PS/PPE, and poly(ethylene oxide) (PEO)/poly(vinylacetate) and PEO/poly(vinylacetate-*ran*-ethylene) blends, are qualitatively consistent with experimental data. But except for PS/PPE and PMMA/PSAN blends, all blends have at least one semi-crystalline polymer or very broad molecular weight distribution. In addition, a PMMA/PSAN blend has a random copolymer and very broad molecular weight distribution. As the study of the viscoelastic properties of an amorphous polymer blend with similar T_g of the constituent component has been reported [22], in this study we employed another amorphous polymer blend of the PS/PVME system, as this has a large difference in T_g between constituent components. Also, this system might be a supplement to the PS/PPE blend system [28]. Although some have recently investigated the rheological properties of PS/PVME blends near the critical temperatures as well as in the homogeneous regime [2–6], a few blend compositions were considered.

In this study, we have investigated in detail the rheological properties of PS/PVME blends covering entire blend compositions in the homogenous regime as well as near the critical regime. The emphasis is placed on investigating whether or not the changes in η_{ob} with blend composition at isothermal conditions are different from those at iso-free volume conditions.

2. Experimental

2.1. Materials

The PS was synthesized via anionic polymerization using a high vacuum apparatus. Cyclohexane was used as the solvent with *sec*-butyl lithium as the initiator, and the reaction temperature was 35°C. The PVME in water solution was purchased from Aldrich Chemical Co. After water was completely removed, PVME was dissolved into toluene (5 wt % of solute) and precipitated using hexane. The weight average molecular weights and molecular weight distributions were 117 000 and 1.06 for the PS, and 94 300 and 1.82 for the PVME. The molecular weight of PS was determined from a calibration curve of monodisperse PS standards, while that of PVME was obtained by a low-angle laser light scattering with the value of $dn/dc = 0.063$ ml/g.

2.2. Sample preparation for rheological measurement

Four blend compositions (10/90, 30/70, 50/50, 70/30 PS/PVME by weight) as well as neat PS and PVME were prepared by dissolving a predetermined amount of polymer in benzene (10 wt % solute in solution) in the presence of an antioxidant (Irganox 1010, Ciba-Geigy Group). The solution was freeze-dried at room temperature for 3 days under vacuum and further dried at $T_g + 40$°C for 2 days under vacuum. The dried sample was compression-molded at $T_g + 70$°C, except for the 70/30 PS/PVME blend which was molded at 100°C, into a sheet of ~ 1 mm in thickness. As the molding temperatures for all blends are lower than the turbidity temperature, all blends are transparent.

2.3. Differential scanning calorimetry (DSC)

The glass transition temperature (T_g) of each blend sample was measured by differential scanning calorimetry (Perkin-Elmer DSC 7 series). Prior to measurement, the baseline was established using two empty pans. To prevent thermal degradation, nitrogen gas was circulated around the sample pan. Each sample of about 15 mg was first heated to $T_g + 50$°C, at a heating rate of 10°C/min, annealed there for 3 min and quenched to $T_g - 50$°C at a cooling rate of 200°C/min. The second heating was used to determine the T_g of the specimen.

2.4. Turbidity temperature measurement

Eight blend compositions for the turbidity temperature (T_b) measurement were prepared by dissolving a predetermined

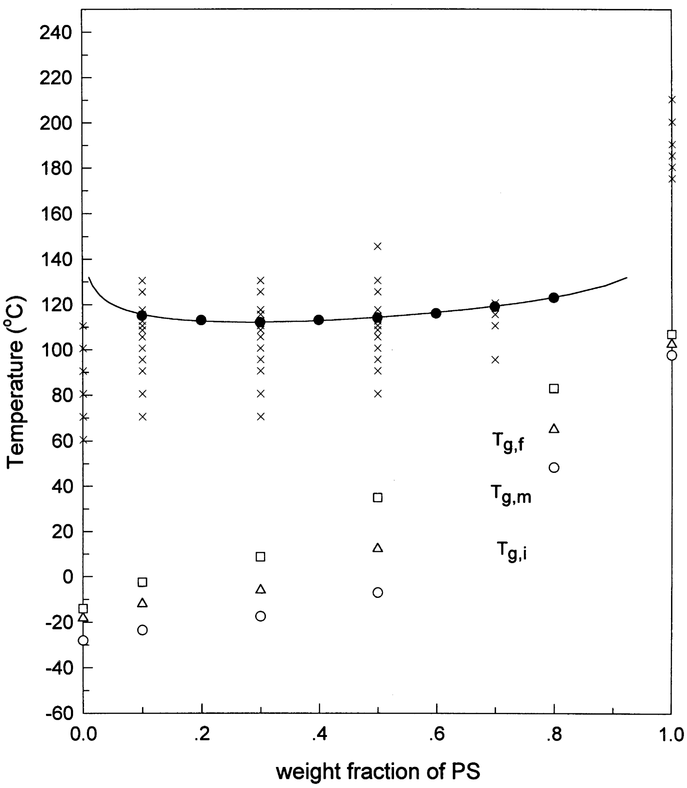

Fig. 1. Composition-dependent cloud points (●) determined from light scattering and glass transition temperatures T_{gi} (○), T_{gm} (△), and T_{gf} (□) for PS/PVME blend employed in this study. The solid line (—) is a binodal curve calculated from curve-fitting experimental data to the Flory–Huggins theory. The symbol (×) denotes temperatures at which rheological properties are measured.

amount of polymer into toluene (10 wt % in solute) and evaporating solvent slowly for 8 h at room temperature. The sample thickness was ~10 μm. The turbidity temperature of each specimen was first estimated by the temperature at which the scattering intensity at the scattering angle of 30° increased abruptly upon heating at a rate of 1°C/min. Then, the T_b of the specimen was determined by the threshold temperature above which the scattering intensity at 30° could be detected, as temperature was increased stepwise with an interval of 1°C from a temperature of 10°C lower than the above estimated value. (e.g. 100°C for 30/70 blend). As the specimen was annealed for 1 h at each temperature, the maximum error in the values of T_b determined would be less than ±1°C.

2.5. Rheological properties measurement

G' and G'' were measured at various temperatures as functions of angular frequency (ω) using an Advanced Rheometric Expanded System (ARES) covering the range of ω from 0.01 to 100 rad/s with 25 mm parallel-plates. Before rheological properties measurement the sample was soaked for at least 30 min at each temperature. Temperature sweep experiments of G' and G'' for various blend compositions were carried out using an ARES at a heating rate of 0.5°C/min and $\omega = 0.5$ rad/s. The strain amplitude (γ_o) for the frequency sweep experiment was 0.05, while that for the temperature sweep experiment was 0.07. Both values of γ_o lay in a linear viscoelastic range.

3. Results and discussion

3.1. Turbidity curve

Fig. 1 gives composition-dependent cloud points (●) determined by LS, composition-dependent glass transitions of the onset point (T_{gi}), the midpoint (T_{gm}), and the final point (T_{gf}), and the temperatures (x) where the rheological properties were measured, for PS/PVME blends employed in this study. From Fig. 1, the blend had a lower critical solution temperature (LCST) of 112 ± 1°C, and the critical weight faction of PS in the blend was 0.3. The interaction energy density (α) in mol/cm^3 was obtained by Flory–Huggins theory and given by [18]:

$$\alpha = 0.478 \times 10^{-3} - (0.176 + 0.0062\phi_{PS})/T \qquad (1)$$

where ϕ_{PS} is the volume fraction of PS in the blend, and T is the absolute temperature. The theoretically predicted binodal curve obtained by Flory–Huggins theory with the aid of Eq. (1) is given as a solid line, from which one notes that the theoretical binodal curve is in good agreement with turbidity results.

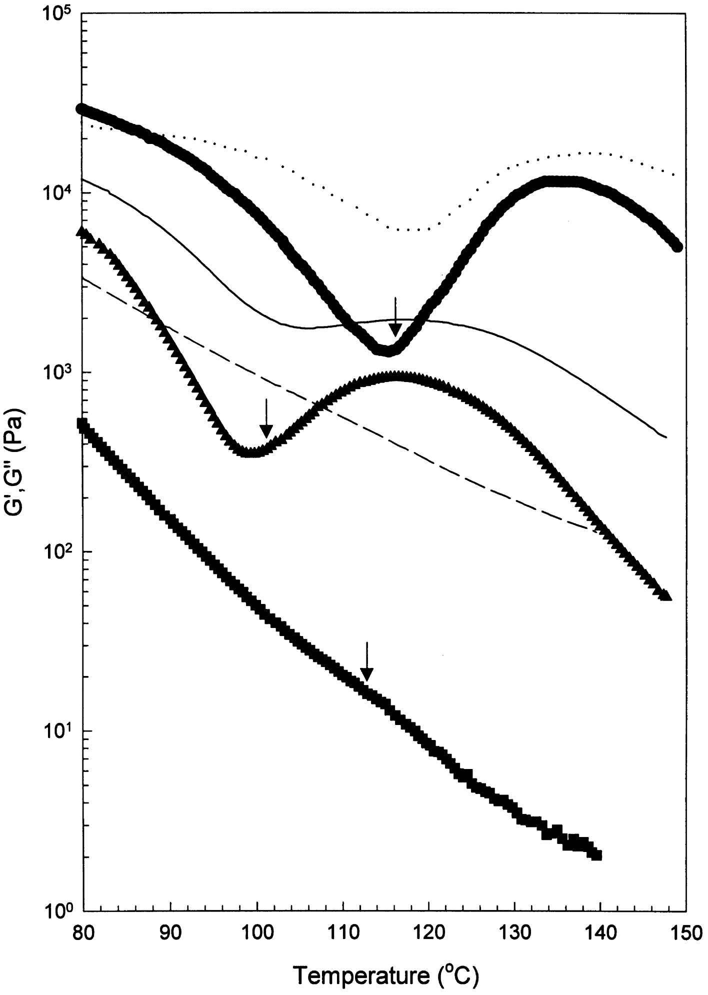

Fig. 2. Temperature sweep of G' (symbols) and G'' (lines) at $\omega = 0.5$ rad/s and $\gamma_o = 0.07$ for the 30/70 (△ and —), the 50/50 (○ and ….) and 10/90 (□ and ---) PS/PVME blends. The onset temperature for the turbidity (T_{in}), above which the turbidity of the sample through the window in a rheometer (RDS-II) could be observed visually, is marked as the arrow(↓) in each G'.

3.2. Miscibility of the blend determined by rheological properties

3.2.1. Temperature sweep experiment

Fig. 2 shows temperature sweep of G' and G'' at $\omega = 0.5$ rad/s and $\gamma_o = 0.07$ for 30/70, 50/50, and 10/90 PS/PVME blends. The onset temperature for the turbidity (T_{in}), above which the turbidity of the sample through the window in a rheometer (RDS-II) could be observed visually during shearing, is marked as the arrow (↓) in each G'. The values of the T_{in} for 30/70, 50/50, and 10/90 PS/PVME blends are 102°C, 116°C, and 113°C, respectively. When we consider the experimental errors in measuring T_{in} and T_b, the values of the T_{in} for the 50/50 and 10/90 PS/PVME blends are essentially identical to those of the T_b. However, the T_{in} for the 30/70 PS/PVME blend is smaller than the LCST (112 ± 1°C) measured by the turbidity method. This is not because of the thickness of the specimens (1 mm) employed in rheometry compared with that (10 μm) employed in LS method. We found that when there was no shear, the turbidity temperature of a thick sample judged by the naked eye was almost the same as the LCST of a thinner sample measured by LS method. This implies that the effect of the oscillatory shear on the turbidity temperature (or shear-induced demixing or phase-separation) was not neglible for the critical composition. Mani et al. [4] reported that a shear-induced mixing and demixing for a PS/PVME blend depended upon the shear rate, shear stress and the blend composition. They found that a shear-induced demixing occurred at temperature as much as 40°C below the LCST. However, the flow type employed in their study was a steady shear. Recently, investigating the effect of oscillatory shear on the demixing process of the blend of polyisoprene and polybutadiene using a large oscillatory shear amplitude ($\gamma_o = 0.8$), Matsuzaka et al. [34] showed that the oscillatory shearing might induced the phase demixing and mixing alternately depending on the phase angle. However, in this study, although a small γ_o (0.07) and $\omega = 0.5$ rad/s were applied to the critical composition of the PS/PVME blend, the shear-induced

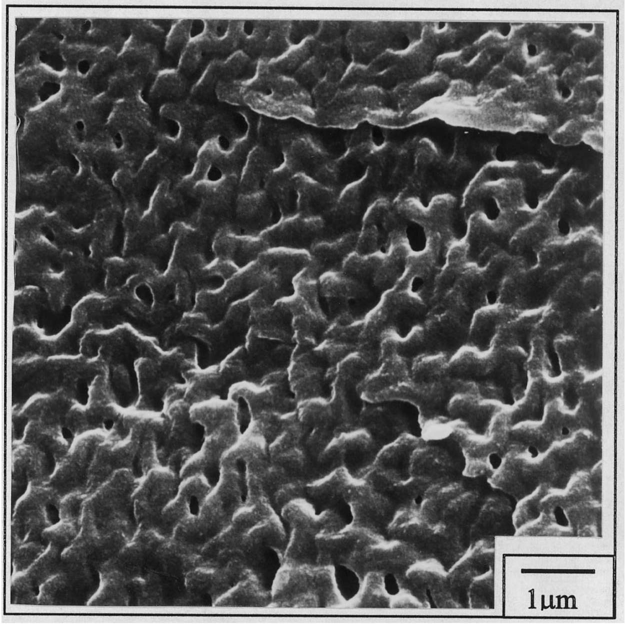

Fig. 3. Field emission SEM image of the 30/70 PS/PVME blend at 105°C while imposing successive oscillatory shearing at $\omega = 0.5$ rad/s and $\gamma_o = 0.07$.

phase-separation (or demixing) was observed even at temperatures as much as 10°C below the LCST obtained without shearing flow. This is attributed to the fact that the concentration fluctuation in the blend found at temperatures corresponding to the homogeneous state but close to the LCST can be accelerated by the oscillatory shearing, thus a shear-induced phase-separation might occur. Once the phase-separation took place, the viscoelastic properties were increased as shown in Fig. 2. As the concentration fluctuation is the largest for the critical composition, the oscillatory shear-induced phase-separation would be small for off-critical compositions such as the 10/90 and 50/50 PS/PVME blends.

In order to investigate whether the shear-induced phase-separation indeed occurred at temperatures lower than the LCST, we observed the morphology of the 30/70 blend by using a scanning electron microscope (Field Emission SEM; Hitachi 301). The sample preparation for SEM was as follows. First, the blend was loaded at 70°C in the rheometer and maintained at this temperature for 30 min. At this moment, the blend was transparent, which was judged visually through the window in the rheometer. Then, the temperature inside the rheometer was increased to 105°C at a rate of 0.5°C/min while successive oscillatory shearing with $\omega = 0.5$ rad/s and $\gamma_o = 0.07$ was imposed to the sample. When the temperature reached 102°C (namely T_{in}), the sample became turbid for the first time. Then, the sample became more turbid as the temperature increased further. When the sample temperature reached 105°C, the oscillatory shearing stopped and the sample was rapidly quenched to a temperature lower than the T_g of this blend by flowing liquid nitrogen into the rheometer. It took less than 10 s to reach this temperature; thus the morphology was successfully fixed as described in a previous paper [19]. Finally, the PVME rich phase in the blend was etched out by methanol for 10 min, then coated with a thin layer of gold.

Fig. 3 gives the SEM image of the 30/70 PS/PVME blend showing clearly the co-continuous structure with a domain spacing of ~0.3 μm, which is similar to phase-separation structure found in the early stage of spinodal decomposition. Previously, we reported that for the 30/70 PS/PVME blends having co-continuous structure with large interdomain spacing (say ~2 μm), the PS-rich phase appeared to be dispersed-phase [19]. However, in this study, the PS-rich phase seemed to be matrix phase. But, the SEM image as shown in Fig. 3 was the overlap image of many layers consisting of PS-rich and etched-out PVME-rich phases having small domain spacing (~0.3 μm). Thus, the PS-rich phase in Fig. 3 should be considered as dispersed-phase.

On the basis of the results given in Figs. 2 and 3, we concluded that the turbidity judged visually was not because of the concentration fluctuation itself, but to the existence of distinct phase-separation resulting from the enhanced concentration fluctuation. This kind of co-continuous structure from the phase-separation definitely increased the modulus. We also found that the sample in the edge of the plates was most turbid because the parallel-plate fixture was employed. However, when the oscillatory shearing stopped at 105°C, the turbid sample returned to be transparent after 4 h. Interestingly, the T_{in} was dependent upon the frequency. For instance, the T_{in} obtained under $\omega = 50$ rad/s and $\gamma_o = 0.07$ was ~106°C, which is 4°C higher than that obtained under $\omega = 0.5$ rad/s and $\gamma_o = 0.07$. The above results led us conclude that the oscillatory shearing also induced a phase-separation for the critical composition of PS/PVME blend.

It can be also seen in Fig. 2 that for the 30/70 PS/PVME blend G' decreased up to 100°C upon heating, as this regime was indeed in the homogenous state. Then, G' and G'' increased up to 118°C with increasing temperature. Interestingly, the temperature of 100°C above which G' increases for the first time was very close to the T_{in}, which is definitely lower than the LCST measured by LS method. This is caused by the shear-induced phase-separation resulting from the enhanced concentration fluctuation in the homogenous regime near the critical temperature, as described already. The increase in moduli with temperature in the range from 100°C to 118°C is attributed to the formation of phase-separated morphology. In addition, the temperature where G' increases for the first time is ~6°C lower than that for G'', and the increase in G' is more evident than that in G''. This suggests that G' becomes more sensitive to the existence of phase-separation than G'' does, which was often found for microphase-separated block copolymers [35–38]. Finally, at higher temperatures where the mobility effect for reducing modulus becomes dominant over the phase-separation effect for increasing modulus, G' and G'' decreased again. Applying the concentration fluctuation

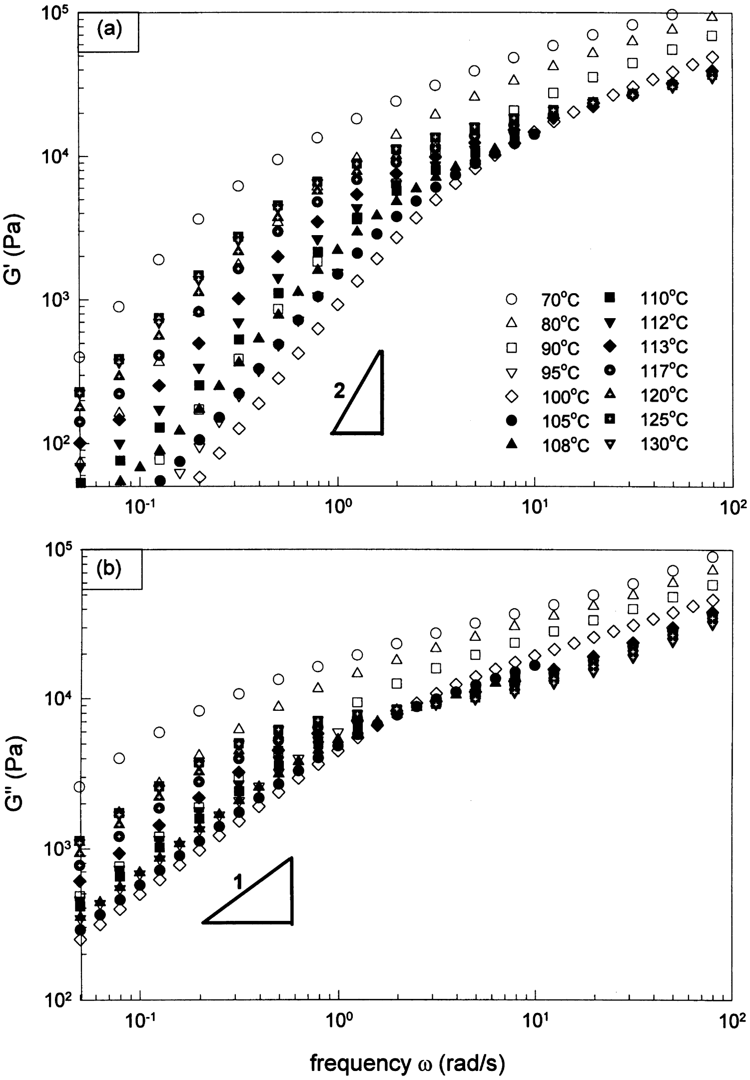

Fig. 4. (a) Log G' versus log ω plots and (b) log G'' versus log ω plots of the 30/70 PS/PVME blend at various temperatures.

concept for a block copolymer developed by Fredrickson and Helfand [39] in a homogenous state near the critical point to polymer blend, the spinodal temperature of the blend can be determined by the plots of $[G''^2/G'T]^{2/3}$ versus $1/T$ [7,40]. The spinodal temperature (T_s) of the 30/70 PS/PVEM blend obtained from this plots was 110°C.

For the 50/50 PS/PVME blend, the moduli change with temperature is very similar to that for the critical blend, namely, the moduli first decrease, then increase, and finally decrease upon heating. The T_s of this blend was estimated to be 135°C from the plots of $[G''^2/G'T]^{2/3}$ versus $1/T$ [7,40]. The estimated T_s was 21°C higher than the T_b (114°C). The difference between the two seems to be too large even if we consider that the former of an off-critical composition should be larger than the latter. Thus, the T_s obtained from this method for a critical composition can be estimated more reliably than that for off-critical compositions, as this method was originally derived for the critical composition of a blend.

However, the moduli change with temperature for the 10/90 PS/PVME blend is quite different from that for the 30/70 and 50/50 blends. For instance, the moduli steadily decreased with temperature even if phase-separation occurred. But the slope of G' versus temperature plots may change at 115°C, although the blend becomes turbid for the first time at 113°C. The steady decrease in the modulus with temperature is as a result of the highly asymmetric blend composition where the rheological properties of the blend with phase-separated morphology are very similar to those of the blend without phase-separated morphology [19].

3.2.2. Frequency sweep experiment

Log G' versus log G'' plots have been widely used for polymer blends, block copolymers, and liquid crystalline polymer [35–37,41]. It is generally known that the blend under investigation becomes homogenous at a specific temperature where these plots do not depend on temperature

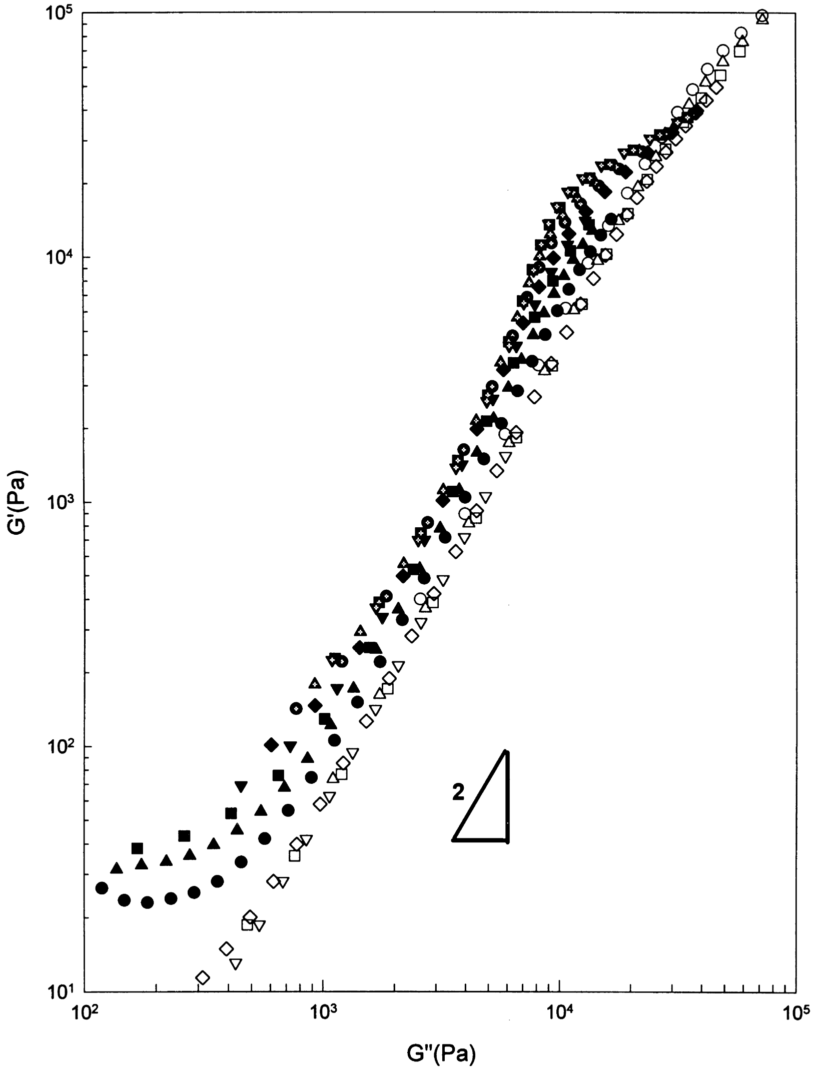

Fig. 5. Log G' versus log G'' plots of the 30/70 PS/PVME blend. Symbols are the same as those in Fig. 4.

any more. Fig. 4 gives log G' versus log ω plots and log G'' versus log ω plots for the 30/70 PS/PVME blend measured from 70°C to 130°C. Using the data given in Fig. 4, we prepared log G' versus log G'' plots, which are given in Fig. 5. It can be seen in Fig. 4 that with increasing temperature G' and G'' at lower values of ω (or at terminal regions) decreased up to 100°C, while the slopes of log G' versus log ω plots and log G'' versus log ω plots are close to two and one, respectively. Then, G' and G'' at lower ω increased and these slopes became smaller. But G' and G'' at higher ω are smaller than those at lower temperatures. These results imply that there is no homogenous state at temperatures larger than 105°C, when judged by rheological properties. This is consistent with the temperature sweep experiment of G' given in Fig. 2.

Log G' versus log G'' plots given in Fig. 5 showed temperature independence up to 100°C and the slope is two in the terminal region. However, these plots at 105°C deviate slightly from those at lower temperatures, although this temperature is still in the homogeneous state based on Fig. 1. Therefore, log G' versus log G'' plots depend on temperatures in the miscible region, as determined from cloud point measurements (see Fig. 1), at temperatures as far away as approximately 7°C below the LCST (112 ± 1°C). One interesting thing to be found in Fig. 5 is that log G' versus log G'' plots do not change much with temperatures ranging from 113°C to 130°C, even when the phase-separated morphology in this regime would be different with temperature. However, as mentioned in our previous paper [19], the phase-separation morphologies at these temperature ranges would be co-continuous morphology when phase-separation time is less than 2 h. Furthermore, as long as co-continuous morphology is maintained, the rheological properties do not change much [19].

Fig. 6 gives log G' versus log G'' plots for the 50/50 PS/PVME blend measured from 80°C to 145°C. The temperature independence was observed up to 112°C and the slope was two in the terminal region, whereas temperature

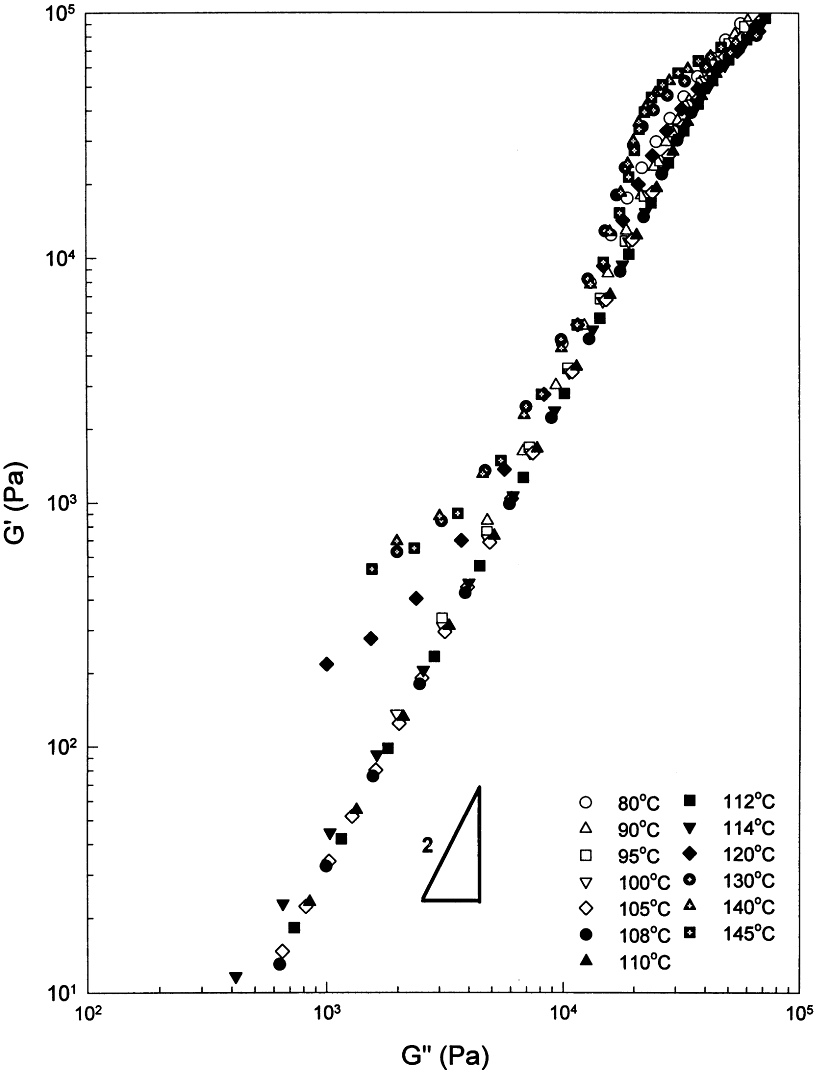

Fig. 6. Log G' versus log G'' plots of the 50/50 PS/PVME blend.

dependence on these plots is first seen at 114°C. These results imply that there is no homogenous state at temperatures higher than 112°C, when judged by rheological properties. This is well consistent with the turbidity result that phase-separated morphology is expected at temperatures higher than the T_b (114°C). This temperature is essentially the same as the T_b given in Fig. 1.

The above observations given in Figs. 5 and 6 are consistent with the results studied by Kapnistos et al. [7]. They reported that log G' versus log G'' plots for a 20/80 PS/PVME blend, which was the critical composition, showed temperature dependence of 3°C–13°C below LCST (93°C), whereas these plots for an off-critical composition (70/30 PS/PVME blend) did not show temperature dependence. They ascribed the temperature dependence of these plots of the critical composition (20/80 PS/PVME blend) to dynamic concentration fluctuations (see Fig. 7 in Ref. [7] near the LCST). But, as described previously, we concluded that this behavior is not because of dynamic concentration fluctuations themselves, rather it is caused by the shear-induced phase-separation (or demixing) at temperatures below but close to the LCST, and this effect was the largest for the critical composition.

Fig. 7 gives log G' versus log G'' plots for the 10/90 PS/PVME blend measured from 70°C to 130°C. Interestingly, log G' versus log G'' plots given in Fig. 7 do not depend on temperatures up to 130°C, which is quite different compared with results given in Figs. 5 and 6. Previously, we [19] reported that when temperature jumped from 105°C (a homogenous regime) to 122°C (a phase-separated regime) for this blend composition, there was no increase (or maximum) in G' and G'' even if phase-separation proceeded. Moreover, G' and G'' did not change with phase-separation time. Even though the phase-separation occurred significantly, thus significantly changing morphology at larger phase-separation times, this change does not affect the modulus much, as rheological properties of 10/90 PS/PVME blend are mainly influenced by the matrix of PVME.

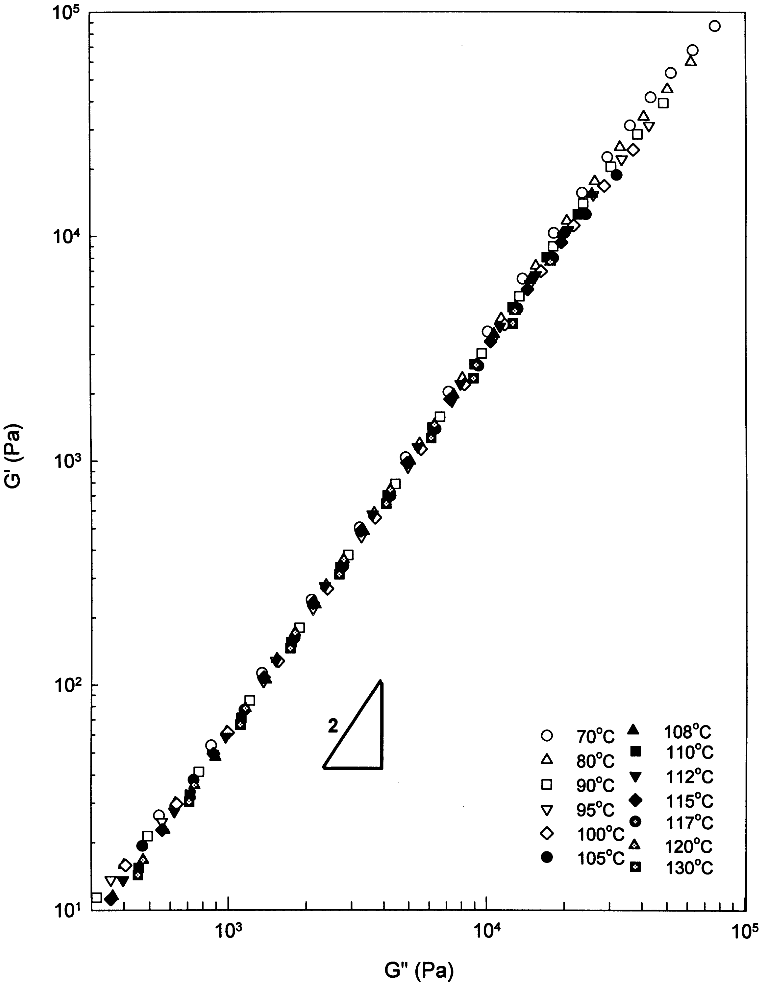

Fig. 7. Log G' versus log G'' plots of the 10/90 PS/PVME blend.

Based on the results given in Figs. 5–7, we can conclude that the T_b for a polymer blend can be unambiguously determined by log G' versus log G'' plots, only when the viscoelastic properties in the phase-separated region are quite different from those in the homogeneous region. However, these plots are not powerful in determining the T_b for a blend where the viscoelastic properties of constituent components are similar and/or a highly asymmetric blend composition. For instance, for a blend with similar viscoelastic properties of constituent components, effects of the existence of the interface or interfacial tension resulting from the phase-separation on G' and G'' would not be large. Bates and coworkers [42] reported that G' and G'' for 50/50 poly(ethylene-*ran*-propylene) (H-PEP which is the hydrogenated 1,4-poly(isoprene))/deuterated PEP (D-PEP) blend do not change with the phase-separation time for up to 5 days at 70°C. This is attributed to the fact that the rheological properties of H-PEP are essentially the same as those of D-PEP at a given temperature, although these two polymers can phase-separate because of the slight positive interaction parameter between the two.

3.3. Rheological properties in the homogeneous region

Fig. 8 gives the change in zero-shear viscosity (η_{ob}) with temperature for PS/PVME blends in the homogenous region as well as neat PS and PVME determined by the turbidity curve based on Fig. 1. All data points for a given composition are well predicted by shift factor (a_T) given in Eq. (2) based on the WLF equation [43] whose constants of C_1 and C_2 are given in Table 1.

$$\log a_T = \frac{-C_1(T - T_{ref})}{[C_2 + (T - T_{ref})]}. \qquad (2)$$

The solid lines in Fig. 8 are predictions based on Eq. (2). Log a_T versus temperature plots for all blend compositions, when the reference temperature (T_{ref}) is fixed at 90°C, are given in Fig. 9(a), while those plots, when the T_{ref} is taken as $T_{gm} + 50°C$, are given in Fig. 9(b). Note that the state employed in Fig. 9(b) (namely, at fixed value of $T - T_{gm}$) is usually regarded as the iso-free volume condition, although this does not necessarily guarantee the iso-free volume condition for a blend consisting of polystyrene

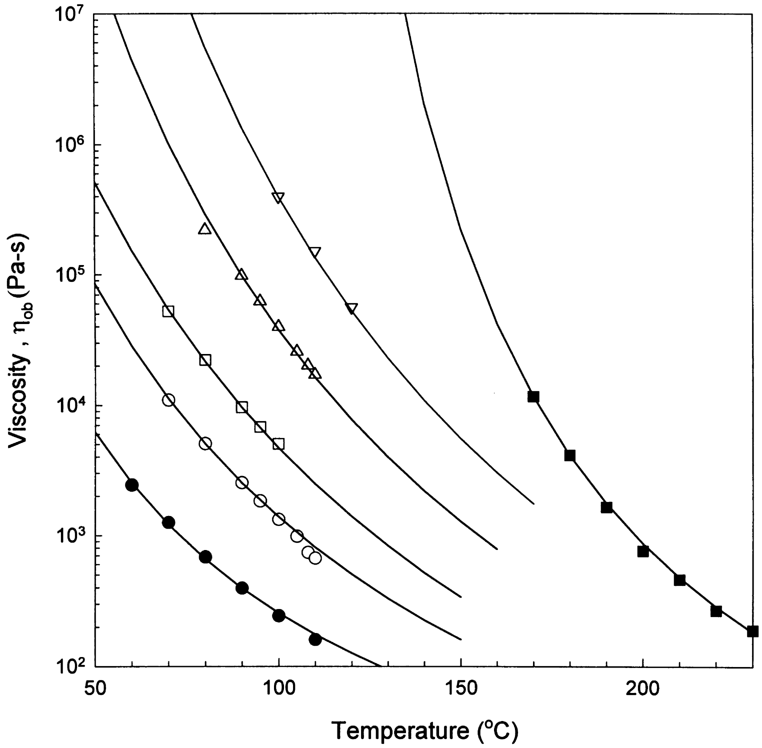

Fig. 8. Zero-shear viscosity (η_{ob}) change with temperature for PS/PVME blends as well as neat PS and PVME in the homogenous region; (●) neat PVME; (○) 10/90 PS/PVME; (□) 30/70 PS/PVME; (△) 50/50 PS/PVME; (▽)70/30 PS/PVME; and (■) neat PS.

and polyisoprene [44]. It can be seen in Fig. 9(b) that log a_T versus temperature plots vary with the blend composition even if the T_{ref} is taken as the fixed value of $T - T_{gm}$. This behavior is more evident as the measuring temperature moves further away from the T_{ref} (namely, at higher temperatures). We found that when the T_{ref} was taken as T_{gi} + 50°C or T_{gf} + 50°C, these plots also varied with the blend composition. Further, we speculated that log a_T versus temperature plots vary with the blend composition even if the exact iso-free volume condition for all compositions is used. The behaviors given in Fig. 9(b) are consistent with results in Refs. [3] and [7]. However, the results given in Fig. 9(b) are at variance with the reports by Aoki [45]. He reported for miscible blends poly(styrene-*co*-N-phenyl maleimide) and poly(styrene-*co*-acrylonitrile) that these plots became independent of blend composition when the T_{ref} was taken as T_{gb} + 50°C, where T_{gb} was taken from the maximum in the tan δ versus temperature curve obtained by a dynamic mechanical thermal analyzer. But these plots depended upon the blend composition when the T_{ref} was fixed at 200°C for all compositions [45]. The reason for the different behavior in those plots at constant distances from the T_g of blend composition between two blend systems is not clear at the present time.

Fig. 10 shows the composition dependence of η_{ob} at constant temperatures of 110 and 120°C. Although all blend compositions employed in this study exhibited phase-separated morphology at 120°C, η_{ob} at 120°C for all compositions are estimated by extrapolation on the basis of Fig. 8 and Eq. (2). It seems that the composition dependence of η_{ob} under isothermal conditions shows negative deviations from linearity, very similar to the previous results reported in the literature [23,27,33]. However, it should be mentioned that a large uncertainty can be incurred in estimating η_{ob} of PS at 110°C and 120°C.

Earlier, several research groups [45–50]suggested the use of iso-free volume conditions (or at temperatures which are at an equal distance from the T_g of the respective blend compositions), instead of isothermal conditions, in investigating composition dependence of η_{ob} of miscible polymer

Table 1
The values of C_1 and C_2 in Eq. (2) for all blend compositions

Blend composition (PS/PVME wt/wt)	C_1	C_2	T_{ref}	Blend composition (PS/PVME wt/wt)	C_1	C_2	T_{ref}
Neat PVME	2.6	127	90	50/50	6.5	147	90
10/90	4.2	150	90	70/30	7.3	147	100
30/70	5.5	167	90	Neat PS	4.5	90	170

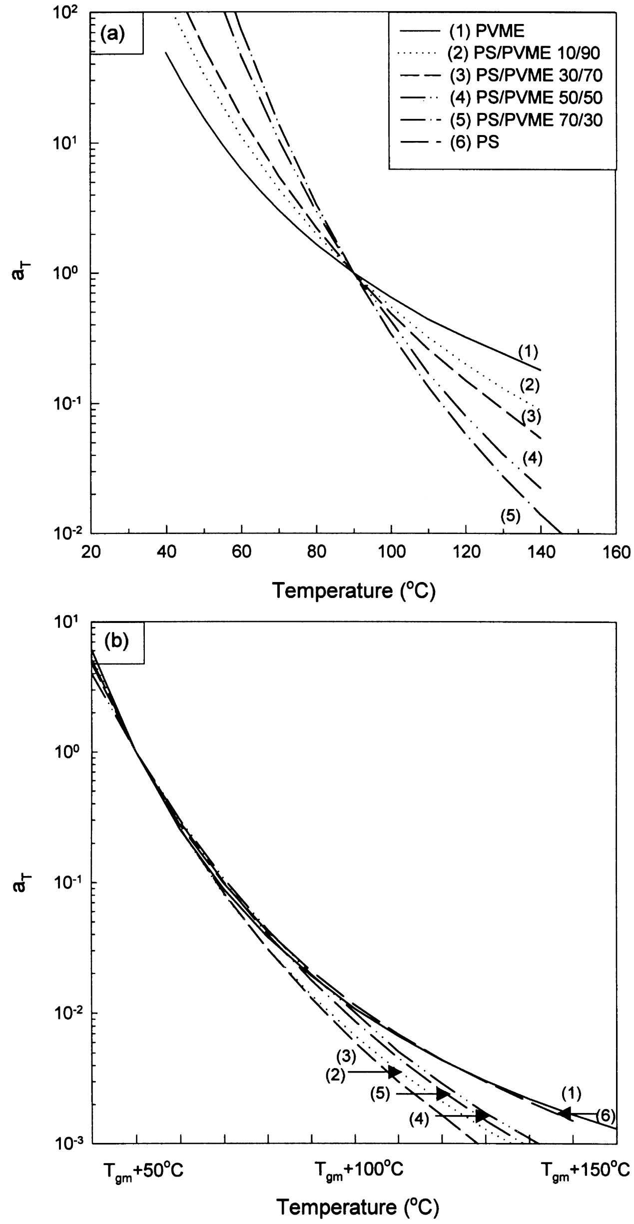

Fig. 9. Log a_T versus temperature plots for all blend compositions: (a) when the T_{ref} is fixed at 90°C and (b) when the T_{ref} is taken as T_{gm} + 50°C.

blends. However, a serious question may be raised as to which of the T_g values (i.e. T_{gi}, T_{gm}, or T_{gf}) should be used when the breadth of glass transition varies significantly with blend composition (see Fig. 1). The composition dependence of η_{ob} is given in Fig. 11(a) at T_{gi} + 80°C, T_{gi} + 90°C, and T_{gi} + 100°C, respectively. It is of interest to observe in Fig. 11(a) that η_{ob} goes through a huge maximum at the 50/50 PS/PVME blend, namely about two orders of magnitude larger than the constituent viscosities. When using T_{gm} as a reference temperature, we observe a slightly different composition dependence of η_{ob}, as given in Fig. 11(b) at T_{gm} + 70°C, T_{gm} + 80°C, and T_{gm} + 90°C, respectively. A maximum in η_{ob} is clearly seen, although the maximum is less than that in Fig. 11(a). We reported a similar behavior for PS/poly(α-methylstyrene) in the homogenous blend [18]. Moreover, the maximum in η_{ob} given in Fig. 11(b) is consistent with results investigated by Green and coworkers [26], although they just employed one blend composition (60/40 PS/PVME). They attributed this behavior to the largest negative value of χ. However, even if the effect χ on η_{ob} was not completely excluded, this effect seems to be too small to explain this huge maximum as the absolute magnitude of χ is on the order of 10^{-3}. Although the exact explanation of the maximum η_{ob} found at a given composition is still unclear, this can be related to the existence of the concentration fluctuation and this was enhanced by an oscillatory shearing flow. Once the enhanced concentration fluctuation (or even the shear-induced phase-demixing) occurred, the friction coefficient of the blend would be larger than that in the completely homogeneous state. As the oscillatory shear-induced concentration fluctuation was the largest for the critical composition as shown in Fig. 2, the critical composition might exhibit the largest viscosity at the iso-free volume condition. It is further noted that when using the temperatures at an equal distance from the T_{gf}, we observed a milder composition dependence of η_{ob} as compared to that shown in Fig. 11. Thus, it is clear from Fig. 11 that the composition dependence of η_{ob} looks different, depending on whether T_{gi}, T_{gm}, or T_{gf} is used as a reference temperature for comparison. This led us to conclude that the dynamics of constituent chains in a PS/PVME blend would not follow the average mobility of the blend at T_{gm}; instead, very complex phenomena between two chains should be considered, as was previously suggested by Zawada et al. [51,52].

Previously, based on the reptation model with the constraint release mechanism, Han and Kim developed a molecular theory [24] that can predict the composition

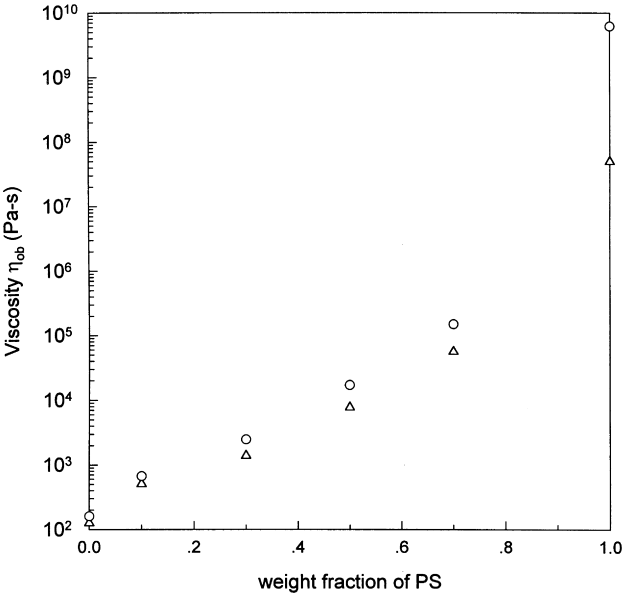

Fig. 10. Composition dependence of η_{ob} at (○) 110°C and (△) 120°C.

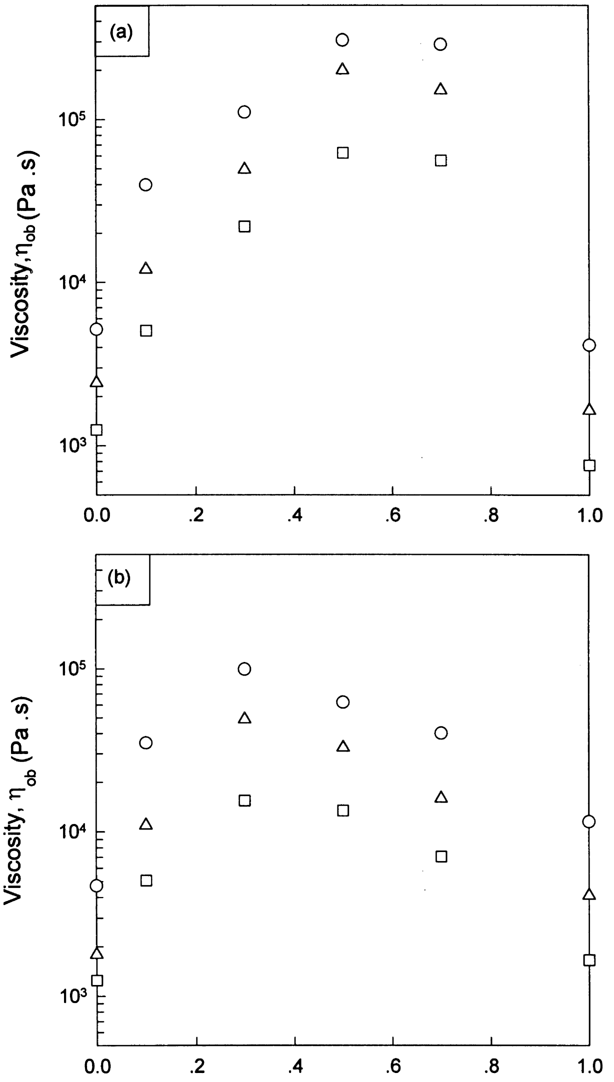

Fig. 11. (a) Composition dependence of η_{ob} at T_{gi} + 80°C (○), T_{gi} + 90°C (△), and T_{gi} + 100°C (□). (b) Composition dependence of η_{ob} at T_{gm} + 70°C (○), T_{gm} + 80°C (△), and T_{gm} + 90°C (□).

dependence of η_{ob} for a miscible blend at the isothermal condition. However, as a result of many uncertainties in estimating the η_o values at 110°C and 120°C for homopolymer PS, we could not apply the above theory for the prediction of the log η_{ob} versus composition plots.

4. Concluding remarks

In this study, we have shown that the rheological properties of PS/PVME blend were dependent upon the blend composition. For the critical composition, $\log G'$ versus $\log G''$ plots show temperature dependence even in the homogenous region determined by LS method, while those plots become temperature independent in the homogeneous region for off-critical compositions. This is because of the oscillatory shear-induced phase-separation and this behavior was most evident for the critical composition.

The logarithmic plots of blend viscosity (η_{ob}) versus composition exhibit a negative deviation at a constant temperature, whereas these show a maximum at a certain composition when the reference temperature is taken as fixed value of $T - T_g$ (under approximately iso-free volume condition). However, we found that the composition dependence of η_{ob} looks different, depending on whether T_{gi}, T_{gm}, or T_{gf} is used as a reference temperature for comparison. This led us to conclude that the dynamics of chains in a PS/PVME blend would not follow the average mobility of the blend at T_{gm}; instead, very complex phenomena between two chains should be considered.

Acknowledgements

This work was supported by the Korean Foundation of Science and Engineering (#97-05-02-03-01-3).

References

[1] Stadler PF, Feitas LL, Krieger V, Klotz S. Polymer 1988;29:1643.
[2] Ajji A, Choplin L, Prud'homme RE. J Polym Sci: Phys Ed 1991;29:1573.
[3] Schneider HA, Wirbser J. New Polym Mater 1990;2:149.
[4] Mani S, Malone MF, Winter HH. Macromolecules 1992;25:5671.
[5] Takahashi Y, Susuki H, Nakagawa, Noda I. Macromolecules 1994;27:6476.
[6] Takahashi Y, Susuki H, Nakagawa Y, Noda I. Polym Int 1994;34:327.
[7] Kapnistos M, Hinrichs A, Vlassopoulos D, Anastasiadis SH, Stammer A, Wolf BA. Macromolecules 1996;29:7155.
[8] Polios IS, Soliman M, Lee C, Gido SP, Schmidt-Rohr K, Winter HH. Macromolecules 1997;30:4470.
[9] Nishi T, Wang TT, Kwei TK. Macromolecules 1975;8:227.
[10] Hashimoto T, Kumaki J, Kawai T. Macromolecules 1983;16:641.
[11] Hashimoto T, Itakura M, Hasegawa H. J Chem Phys 1986;16:6118.
[12] Yang H, Shibayama M, Stein RS, Shimizu N, Hashimoto T. Macromolecules 1986;19:1667.
[13] Okada M, Han CC. J Chem Phys 1986;85:5317.
[14] Han CC, Okada M, Muroga Y, Bauer BJ, Tran-Cong Q. Polym Eng Sci 1986;26:1208.
[15] Shibayama M, Yang H, Stein RS, Han CC. Macromolecules 1985;18:2179.
[16] Fernamdez ML, Higgins JS, Horst R, Wolf BA. Polymer 1995;36:149.
[17] Fernamdez ML, Higgins JS, Richardson SM. Polymer 1995;36:931.
[18] Kim JK, Lee HH, Son HW, Han CD. Macromolecules 1998;31:8566.
[19] Kim JK, Son HW, Lee YB, Kim J. J Polym Sci: Polym Phys Ed 1999. In press.
[20] Wu S. J Polym Sci: Polym Phys Ed 1987;25:557, 2511.
[21] Wu S. Polymer 1987;28:1144.
[22] Friedrich C, Schawarzwalder C, Riemanm RE. Polymer 1996;37:2499.
[23] Han CD, Kim JK. Macromolecules 1989;22:1914.
[24] Han CD, Kim JK. Macromolecules 1989;22:4292.
[25] Yang HH, Han CD, Kim JK. Polymer 1994;35:1503.
[26] Green PF, Adolf DB, Gilliom LR. Macromolecules 1991;24:3377.
[27] Han CD, Yang HH. J Apply Polym Sci 1987;33:1199.
[28] Kim JK, Han CD, Lee YJ. Polymer J 1992;24:205.
[29] Roover J, Toporowski PM. Macromolecules 1992;25:1096, 3454.

[30] Ougizawa T. Polymer Prep (Japan) 1990;39:1217.

[31] Ougizawa T, Dee GT, Walsa DJ. Polymer Prep (Japan) 1990;39: 3539.

[32] Personal Communication with Ougizawa T (Sept 1998).

[33] Han CD, Chung HS, Kim JK. Polymer 1992;33:546.

[34] Matsuzaka K, Jinnai H, Koga T, Hashimoto T. Macromolecules 1997;30:1146.

[35] Han CD, Kim JK. Polymer 1993;34:2533.

[36] Han CD, Baek DM, Kim JK. Macromolecules 1990;23:561.

[37] Han CD, Baek DM, Kim JK, Ogawa T, Hashimoto T. Macromolecules 1995;28:5043.

[38] Bates FS. Macromolecules 1984;17:2607.

[39] Fredrickson GH, Helfand E. J Chem Phys 1987;87:697.

[40] Ajji A, Choplin L. Macromolecules 1991;24:5221.

[41] Kim SS, Han CD. Macromolecules 1993;26:6633.

[42] Kedrowski C, Bates FS, Eiltzius P. Macromolecules 1993;26:3448.

[43] Ferry JD. Viscoelastic properties of polymers. New York: Wiley, 1980.

[44] Chapman BR, Hamersky MW, Milhaupt JM, Kostelecky C, Lodge TP, von Meerwall ED, Smith SD. Macromolecules 1998;31:4562.

[45] Aoki Y. Macromolecules 1990;23:2309.

[46] Roland CM, Ngai KL. Macromolecules 1991;24 2261:5315.

[47] Chung G-C, Kornfield JA, Smith SD. Macromolecules 1994;27:964, 5729.

[48] Arendt BH, Krishnamoorti R, Kannan RM, Zawail M, Kornfield JA, Smith SD. Polym Mater Sci Eng 1994;71:471.

[49] Kim E, Kramer EJ, Osby JO. Macromolecules 1995;28:1979.

[50] Kim E, Kramer EJ, Wu W, Garrett PD. Polymer 1994;35:5706.

[51] Zawada JA, Ylitalo CM, Fuller GG, Colby RH, Long TE. Macromolecules 1992;25:2896.

[52] Zawada JA, Fuller GG, Colby RH, Fetters LJ, Roover J. Macromolecules 1994;27:6851–6861.